Yield Estimation of a Memristive Sensor Array

Vishal Gupta*, Saurabh Khandelwal†, Giulio Panunzi*, Eugenio Martinelli*,
Said Hamdioui§, Abusaleh Jabir† and Marco Ottavi*
*Department of Electronic Engineering, University of Rome "Tor Vergata", Italy.
Email: {vishal.gupta, giulio.panunzi}@students.uniroma2.eu, {martinelli, ottavi}@ing.uniroma2.it
†School of ECM, Oxford Brookes University, UK. Email: {skhandelwal, ajabir}@brookes.ac.uk
§Quantum and Computer Engg., Delft University of Technology, Netherlands. Email: s.hamdioui@tudelft.nl

***Abstract*—This paper proposes a method to calculate the yield of a memristor based sensor array considered as the probability that the chip provides acceptable sensing results when the array is affected by manufacturing defects. The modeling is based on a Markov Chain approach, in which each state represents an operating chip configuration and the state transitions take into account manufacturing defects. The proposed method is applicable to evaluate the yield with different fault models to achieve the comparative yield obtained by several redundancy allocations.**

***Index Terms*—Memristor, Gas Sensor, Markov Modeling, Yield, Redundancy**

I. Introduction

A typical structure of TiO_2-based memristor proposed by HP Labs [1] is shown in Fig. 1a. Semiconducting metal oxide based memristors are used as gas sensor [2], the main cause of change of the sensor's resistance is due to the loss (gain) of the free charge carriers (electrons or holes) from (to) the semiconductor to (from) its surface [2]. The initial and final resistances of the device after gas exposure are measured and the gas properties of such gas are determined from the measured values [3]. Gas sensing can be prone to yield and reliability issues due to defect/faults in the device itself [4], [5]. The goal of the paper is to introduce and analyze a highly accurate method for estimating the yield of memristor based gas sensor arrays and the benefits of repair mechanisms through a Markov-based analysis. This approach provides a high level of effectiveness and accuracy with respect to the industrial design data for the defects. To reduce the complexity of the allocation algorithm, only one-dimensional redundancy (spare rows) has been considered in this paper.

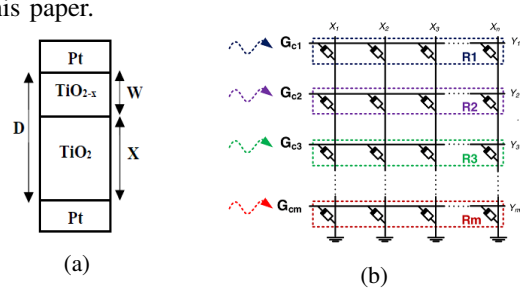

(a) (b)

Fig. 1: (a) Structure of the TiO_2-based memristor fabricated by HP Labs [1]. (b) Multi-gas with m(1xn) sensing array configuration [3].

II. Defects Modelling & Impact on Sensing

Markov chain model [6] has been applied to the specific row sensing scheme as shown in Fig. 1b to estimate the yield. This configuration offers a combined response equivalent to the parallel combination of the memristor based gas sensors. The sensing structure depicted in Fig. 1b makes it possible to introduce a repair mechanism that addresses the faulty sensors in the array. This can be achieved by checking if the response of a memristor (sensor) considerably differs from the rest, in such case, the row can be substituted depending on the type of fault present. In this paper, we have considered open (λ_{sco}) and short (λ_{scs}) single cell faults. Unlike a short fault, an open fault is acceptable for each row before initiating the replacement of the rows if the equivalent resistance is within the expected accuracy. The repair process of the Markov chain model can be described as a series of states representing the different configurations of the gas sensor, depending on the number of faults that have been repaired.

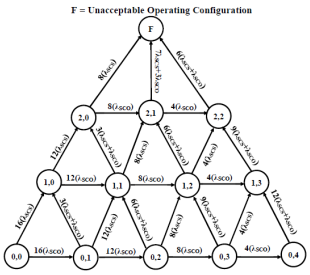

(a)

```
for k = 1 to n_max do
    P = P_0 × A^k;
    G(k) = P(1);
    for m = 2 to ((n_r + 1) × 2) − 1 do
        if mod(m,2) == 0 then
            G(k) = G(k) + P(m);
        end if
    end for
    Y(k) = 1 − P(((n_r + 1) × 2) + (n_r − 1));
end for
```

(b)

Fig. 2: (a) Markov chain state transition diagram for the 4×4 gas sensor array. Here, first term (i) & second term (j) of each operating configurations is indicating the number of spare rows used and the number of acceptable faults that have occurred respectively. (b) Algorithm for computation of yield.

Fig. 2a is the state transition diagram showing reconfiguration strategy that reorganises the fault free cells in a 4×4 gas sensor array having two spare rows and one acceptable fault in all the n_r rows of the array. Circles denote the chip operating configurations (OC's). Each OC state corresponds to the level of redundancy currently available in the gas sensor array and the acceptable faults in each row. The occurrence of a fault causes a state transition to the corresponding gas sensor configuration after (possibly) performing a repair operation. Chip unacceptable operating configuration are aggregated into a single "absorbing state (F)". This is the faulty state in which the chip has to be discarded. It is reached either when a fault hits some unreconfigurable circuit or when the number of spare rows is completely exhausted. The proposed repair algorithm processes faults one at a time. The state-to-state transitions are governed by the following events (assuming that we are in state (0,0) and we have n_c=4, n_r=4, spare rows (r)=2, where n_c and n_r denote the number of columns and rows respectively).

i. A *sco* type of fault hits a single cell out of n_c×(n_r+r)

active ones. Then, if *sco* $\leq$ one fault in all the n_r rows of the array, transition takes place from one *OC* state to another *OC* state without replacing the word line. Otherwise the corresponding word line is replaced.

ii. A *scs* type of fault hits a single cell out of $n_c \times (n_r+r)$ active ones. Then, the faulty line is replaced by a spare word line.

The transition rates and the weighted sum of all possible faults causing the transition for the Markov chain model are shown in Table I. The values of the fault rates are divided by either the number of columns or rows (or their product). This is because all the faults are assumed to be independent and their weighted probabilities are assumed when characterizing a transition rate [6]. The transition rates reported in Table I can be interpreted with the following example: Consider the transition rate $\lambda_{00,10}$ from a state with no allocated spare row to a state with only one allocated spare row. In this case, the transition rate is given by the term.

- $\lambda_{scs}(n_c(n_r\text{-}(n\text{-}1)))$: This is the probability of having short single cell fault in any of the $n_c \times n_r$ cells of the array. Here $(n-1)$ is indicating number of rows with fault. For this transition n=1.

Yield for the example shown in Fig. 2a is computed by the Algorithm shown in Fig. 2b. Here, $P = P_0 \times A^k$ is the generating matrix representing the probability of transition from state (0, 0) to other acceptable states and the absorbing state (F), n_r=4, k is the average defect rate, P_0 is the initial state distribution matrix, A^k is the generating matrix after k^{th} defect, $G(k)$ represents the yield of the chip with no spare row and $Y(k)$ represent the yield of the chip with 2 spare rows.

TABLE I: Defect Intensities

Transition Rates		Weighted sum of all possible faults causing the transition
OC's (0,n) to (0,n+1)	$\lambda_{0n,0(n+1)}(n)$	$\lambda_{sco}(n_c(n_r\text{-}(n\text{-}1)))$
OC's (0,n) to (1,n)	$\lambda_{0n,1n}(n)$	$\lambda_{scs}(n_c(n_r\text{-}(n\text{-}1)))$
OC's (0,n) to (1,n-1)	$\lambda_{0n,1(n-1)}(n)$	$(\lambda_{scs}+\lambda_{sco})(n\text{-}1)(n_c\text{-}1)$
OC's (1,n) to (1,n+1)	$\lambda_{1n,1(n+1)}(n)$	$\lambda_{sco}(n_c((n_r\text{-}1)\text{-}(n\text{-}1)))$
OC's (1,n) to (2,n)	$\lambda_{1n,2n}(n)$	$\lambda_{scs}(n_c((n_r\text{-}1)\text{-}(n\text{-}1)))$
OC's (1,n) to (2,n-1)	$\lambda_{1n,2(n-1)}(n)$	$(\lambda_{scs}+\lambda_{sco})(n\text{-}1)(n_c\text{-}1)$
OC's (2,n) to (2,n+1)	$\lambda_{2n,2(n+1)}(n)$	$\lambda_{sco}(n_c((n_r\text{-}2)\text{-}(n\text{-}1)))$
OC's (2,n) to (F)	$\lambda_{2n,f}(n)$	$\lambda_{scs}((n_c(n_r\text{-}2))\text{-}(n\text{-}1))$ $+\lambda_{sco}((n\text{-}1)(n_c\text{-}1))$

III. Results and Discussion

The proposed Markov model was coded and tested in MATLAB. The solution is based on matrix multiplications and the number of matrix multiplications to solve is related to the required accuracy (which is higher for the lower values of the execution step $\Delta\lambda$) and the maximum value of the average fault number. In Fig. 3a and Fig. 3b, simulation results are shown for a 4×4 gas sensor array by varying the average defect rate from 0 to 30 with a step $\Delta T = 10^{-3}$. For Fig. 3a, the short and open single cell faults is considered to be $\lambda_{scs} = \lambda_{sco} = \frac{0.5}{n_c n_r}$ and the simulation result shows that yield of the gas sensor array with two spare rows is higher than the gas sensor array with no spare rows. Fig. 3b shows the yield comparison with varying percentage of open and short single cell faults considering $r = 2$ and the acceptable number of faults in all the n_r rows of the array = 1 and $\Delta\lambda = 10^{-3}$. The following defect ratios were plotted: C1:$\lambda_{sco}=\frac{0.9}{n_c n_r}$, $\lambda_{scs}=\frac{0.1}{n_c n_r}$; C2:$\lambda_{sco}=\frac{0.7}{n_c n_r}$, $\lambda_{scs}=\frac{0.3}{n_c n_r}$;C3:$\lambda_{sco}=\frac{0.5}{n_c n_r}$, $\lambda_{scs}=\frac{0.5}{n_c n_r}$; C4:$\lambda_{sco}=\frac{0.3}{n_c n_r}$, $\lambda_{scs}=\frac{0.7}{n_c n_r}$; C5:$\lambda_{sco}=\frac{0.1}{n_c n_r}$, $\lambda_{scs}=\frac{0.9}{n_c n_r}$. The simulation results show that the higher the percentage of the open single cell faults compared to short single cell faults, the higher the yield. This is quite an interesting result which emphasises the difference of this structure with respect to conventional memory arrays: in fact in this case the final yield is not only a function of the overall defect rate but also of the specific defect type that is prevalent in the array.

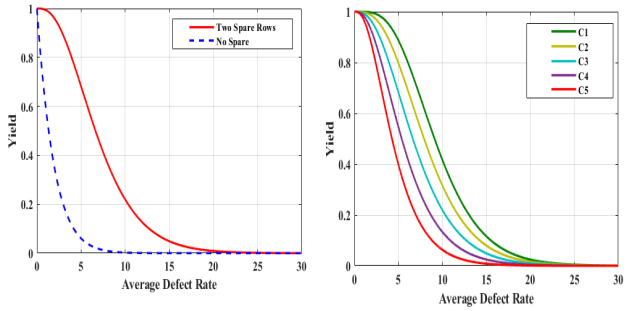

(a) (b)

Fig. 3: A yield comparison varying defect rate for a 4×4 gas sensor array: (a) for $\lambda_{scs} = \lambda_{sco} = \frac{0.5}{n_c n_r}$. (b) for different percentages of λ_{scs} & λ_{sco} as discussed in Section III.

IV. Conclusions

In this paper, we developed a model to estimate the yield of memristor based gas sensor array with/without redundancy. The model takes into account the types of defects/faults, derive the state-to-state transition probabilities and creates the generating matrix to compute the yield. Using this model, a $4\cdot(1\times4)$ multi-gas sensor array configuration has been investigated for yield evaluation considering two spare rows and one acceptable fault in all the n_r rows of the array. Yield is shown to be higher with redundancy as well as with higher probability of having open single cell fault compare to short single cell fault. The proposed model is flexible and can be modified to include observed faults from manufactured devices.

Acknowledgment

The work was funded by the Leverhulme Trust Research Project Grant, under Grant No.RPG-2017-344.

References

[1] R. S. Williams, "How we found the missing memristor," *IEEE Spectrum*, vol. 45, no. 12, pp. 28–35, 2008.

[2] A. A. Haidry, A. Ebach-Stahl, and B. Saruhan, "Effect of pt/tio2 interface on room temperature hydrogen sensing performance of memristor type pt/tio2/pt structure," *Sensors and Actuators B: Chemical*, vol. 253, pp. 1043 – 1054, 2017.

[3] A. Adedotun, J. Mathew, A. Jabir, C. D. Natale, E. Martinelli, and M. Ottavi, "Efficient sensing approaches for high-density memristor sensor array," *Journal of Computational Electronics*, vol. 17, no. 3, pp. 1285–1296, 2018.

[4] S. Khandelwal, A. Bala, V. Gupta, M. Ottavi, E. Martinelli, and A. Jabir, "Fault modeling and simulation of memristor based gas sensors," in *2019 IEEE 25th International Symposium on On-Line Testing and Robust System Design (IOLTS)*, pp. 58–59, July 2019.

[5] M. Ottavi, V. Gupta, S. Khandelwal, S. Kvatinsky, J. Mathew, E. Martinelli, and A. Jabir, "The missing applications found: Robust design techniques and novel uses of memristors," in *2019 IEEE 25th International Symposium on On-Line Testing and Robust System Design (IOLTS)*, pp. 159–164, IEEE, 2019.

[6] M. Ottavi, L. Schiano, X. Wang, Y. . Kim, F. J. Meyer, and F. Lombardi, "Evaluating the yield of repairable srams for ate," *IEEE Transactions on Instrumentation and Measurement*, vol. 55, no. 5, pp. 1704–1712, 2006.